Journal of Applied Fluid Mechanics, Vol. 17, No. 12, pp. 2720-2733, 2024.
Available online at www.jafmonline.net, ISSN 1735-3572, EISSN 1735-3645.
https://doi.org/10.47176/jafm.17.12.2611

Increasing L/D Ratio of Wing by Delaying Flow Separation for Better Aerodynamic Performance

J. P. Ramesh[1†], V. Mugendiran[2] and G. Sivaraj[3]

[1] *Department of Mechanical Engineering, SRM Valliammai Engineering College, Kanchipuram, Tamilnadu, 603203, India*
[2] *Department of Production Technology, Anna University (MIT) Campus, Chennai, Tamilnadu, 600044, India*
[3] *Subsonic Airflow Testing Facility, Research Park, Bannari Amman Institute of Technology, Erode, Tamilnadu, 638401, India*

†*Corresponding Author Email: rameshp.mech@srmvalliammai.ac.in*

ABSTRACT

To improve the aerodynamic efficiency of the aircraft, the article focuses on optimizing *the L/D* ratio through postponement of flow separation. Elevating the L/D ratio leads to diminished drag and delays stall occurrence at high angles of attack (α). The wing geometry adopts NACA 6-digit airfoils, specifically NACA 63418 and NACA 63415. Various aerodynamic devices are explored for their ability to defer flow separation, with passive aerodynamic devices being the prevalent choice. The primary goal of the research is to integrate rotational thin wire elements into the aerodynamic components of the wing, aiming to diminish drag, amplify lift, and enhance overall aerodynamic performance. The analysis spans a range of α, from 0° to 20°. The study encompasses two scenarios: one without the incorporation of aerodynamic devices and the other with their implementation. Comparative analyses of increases in C_L and reductions in C_D, with notable improvements observed at a 15° angle of attack, 28.47% increase in C_L and 15.07% decrease in C_D. Furthermore, the improved performance in the C_L/C_D, which increases substantially in stall conditions, thereby demonstrating the potential of these aerodynamic modifications to enhance overall aircraft performance.

Article History

Received January 25, 2024
Revised June 9, 2024
Accepted June 17, 2024
Available online October 2, 2024

Keywords:

Boundary layer
Flow separation
Drag force
Lift force
Circulation

1. INTRODUCTION

There have been several aircraft accidents that have been attributed, at least in part, to flow separation. Flow separation is a phenomenon in aerodynamics where the boundary layer of air over a surface separates from the surface, resulting in a loss of lift or increased drag. Flow separation occurs when the air flowing around the surface of an aircraft's wing detaches from surface and forms a turbulent wake, instead of following the contour of the airfoil. This can lead to a loss of lift and increased drag, which can affect the performance and stability of the aircraft. The flow of air over an airfoil is affected by various factors such as the angle of attack, the shape of the airfoil, and the speed of the air. If the α is too high or the speed of the air is too low, the flow of air can become turbulent, causing separation of the boundary layer from the surface of the airfoil. To prevent flow separation, designers of aircraft airfoils may use various techniques, such as shaping the airfoil to produce smooth, streamlined flow, adding devices such as vortex generators to energize the flow, and using active flow control techniques such as blowing or suction to maintain smooth flow over the airfoil. Here are a few examples of aircraft accidents that have involved flow separation:

1. DHC – Q400: On June 1, 2009, a Bombardier operating as DHC – Q400 crashed into the Buffalo, New York. The crash was caused by a combination of factors, including a loss of airspeed data due to ice crystals in the pitot tubes and wings and the crew's inappropriate response to the resulting stall. The investigation found that flow separation on the plane's wings contributed to the stall.
2. China Airlines Flight 140: On April 26, 1994, a Boeing 737-300 operating as China Airlines Flight 140 crashed while landing in Nagoya, Japan. The accident was caused by the crew's failure to perform the correct landing procedures, which resulted in the plane's wing flaps being extended too early. This caused flow separation on the wings, leading to a loss of lift and a subsequent crash.
3. American Airlines Flight 587: On 12th Nov 2001, an Airbus A300-600 operated by American Airlines crashed into a residential area in Queens, New York,

shortly after takeoff. The cause of the accident was attributed to the failure of the vertical stabilizer due to excessive rudder inputs by the first officer, which resulted in flow separation and the separation of the tail section from the plane.

1.1 Flow Separation

Flow separation is a phenomenon in aerodynamics where the boundary layer of air over a surface separates from the surface, resulting in a loss of lift or increased drag. Here are some of the common causes of flow separation in aircraft: Stalling at high angle of attack, the flow over the wings can become turbulent at high speed leading to flow separation, wingtip vortices, contamination of ice, snow and etc., Flow separation is a complex phenomenon that can be affected by many factors. Aircraft designers and engineers use a variety of techniques, such as wind tunnel testing and computer simulations, to design and test airfoils and other components to minimize the risk of flow separation.

Flow separation occurs when the flow of a fluid detaches from a surface, causing a loss of lift and an increase in drag. To delay flow separation, the following methods can be used: install vortex generator, use boundary layer control, add suction, and smooth the surface. These methods are commonly used in various industries, including aerospace, automotive, and marine engineering, to delay flow separation and improve the performance of aerodynamic surfaces.

Shan et al. (2008) conducted a numerical investigation into subsonic flow separation over a NACA0012 airfoil at a 6˚ angle of attack, employing the immersed boundary method. This study, which included three simulations, focused on flow separation control using vortex generators (VGs). The results indicated that the implementation of passive VGs can partially eliminate flow separation, suggesting their effectiveness in enhancing aerodynamic performance. Building upon this, Manolesos et al. (2015) conducted computational research on the application of co-rotating blade-type vortex generators on transonic sweptback wings. The study meticulously analyzed how the incident angle of the vortex generators interacts with local airflow to enhance the aerodynamic performance of the wings. The effectiveness of the vortex generators was compared with that of a common research model, demonstrating that they perform comparably to an infinite span wing at moderate sweep angles. The results underscore the potential of co-rotating blade-type vortex generators in improving lift and delaying flow separation on sweptback wings. Similarly, Wang et al. (2017) explored the effectiveness of vortex generators as passive flow control devices aimed at enhancing the aerodynamic performance of large wind turbines. Their study focused on the S089 airfoil, demonstrating that vortex generators can significantly influence the aerodynamic characteristics by reducing the boundary layer thickness and delaying stall. The findings affirm that the strategic application of vortex generators on wind turbines not only optimizes performance but also delivers substantial aerodynamic benefits.

Further refinement in VG applications was explored by Ito et al. (2016), who investigated the dynamics of strong turbulence between two vortices at a downstream height of 37.2 VGs. Their study focused on analyzing the interactions facilitated by the wandering motion of vortex generators (VGs) located between these vortices. The findings revealed that this motion significantly increases the normal stress between the vortices, indicating a profound effect of VG positioning on turbulence behavior. Anand et al. (2010) further augmented this line of research, who conducted comprehensive numerical simulations to assess the impact of vortex generators (VGs) on a NACA0012 aerofoil at a wide range of attack angles, with a Reynolds number of 5.5×10^5. Utilizing FLUENT software, they solved the three-dimensional Reynolds-averaged Navier-Stokes equations alongside the Spalart-Allmaras turbulence model. Their findings indicate that VGs significantly enhance aerodynamic performance by increasing the lift coefficient and reducing the drag coefficient, particularly at high angles of attack. The study underscores the role of VGs in modifying fluid flow and aerodynamic forces, effectively delaying the onset of stall and improving overall aerofoil efficiency.

Further investigations by Yangwei et al. (2017) conducted a systematic study on the effects of placing a small plate near the leading edge of an airfoil to mitigate increasing drag and decreasing lift in fluid flow. Their findings revealed that at Mach number 0.5, this setup resulted in a significantly higher lift coefficient, even at large angles of attack; however, at Mach numbers above 0.5, the improvement in airfoil performance was less pronounced. Building on the theme of surface modifications, Merryisha & Rajendran (2019) explored how variations in surface roughness could influence aerodynamic characteristics. Their research determined that increasing the roughness of the airfoil's surface at certain angles of attack effectively reduces drag formation. This modification also enhances stalling characteristics, thereby improving landing efficiency and aircraft stability. The experimental outcomes indicated that different types of surface modifiers contribute variably to wake divergence factors. These factors are crucial in elevating the stall angle and thus restricting the aircraft under specific flight conditions.

In a series of recent studies focusing on vortex generators (VGs), researchers have advanced our understanding of their aerodynamic impacts under various conditions. Ichikawa et al. (2021) conducted wind tunnel tests to evaluate the influence of the size of rectangular vane-type VGs on the lift force of a model featuring a half-span high-lift swept-back wing, with experiments performed at a Reynolds number of 1.86×10^5 in a low-speed environment. Their findings highlight the sensitive relationship between VG dimensions and aerodynamic performance.

Further exploring the design optimization of VGs, Namura et al. (2019) employed computational fluid dynamics to execute a multipoint design optimization focusing on VG shape and placement on swept wings. Their optimization process was conducted in two stages: initially optimizing the VG shape on an infinite swept

wing using a cross-sectional airfoil from the Common Research Model (CRM), followed by refining the VG arrangement using the comprehensive NASA CRM. This approach allowed for designs that are adaptable for both cruising and critical flight scenarios. Saraf et al. (2018) and Mahboub et al. (2022) have studied the help of vortex generators in reducing pressure drag on the external surface for flow separation is massive. As the drag and lift of the airfoil depends on the linearity of the foil any bump can change the geometry of the foil thus changing the aerodynamic performance. An analysis found that flow separation can delay bump formation and the vortex generator can re-energize the flow hence reducing the pressure drag.

Additionally, Wik and S. Shaw (2004) explored the aerodynamics of micro-vortex generators through computational studies. They used incompressible Reynolds-Averaged Navier-Stokes equations to study a rectangular vane-type micro-VG placed on a flat plate at a Reynolds number of 81,000. Their research underscores the critical need for precise resolution in simulations, particularly concerning the thickness and boundary layer treatment of VGs. They demonstrated that neglecting these factors can lead to significant discrepancies between computational predictions and experimental results, emphasizing the importance of accurate modeling in aerodynamic research.

Lastly, Kusunose and Yu (2003) investigated the effect of the boundary layer's expansion along the wing surface on the drag induced by a vortex generator (VG) blade. They demonstrated that the drag increases as the boundary layer expands with distance along the wing. Concurrently, Nash and Bradshaw criticized the conventional method of using the ratio of local to freestream dynamic pressure to approximate the magnification (q effect) of drag. They introduced a novel magnification factor formula to evaluate VG-induced drag more accurately in transonic-transport airplane models. Their approach facilitated several assessments of VG installation, revealing that the magnification effect was previously overestimated. The results from wind-tunnel tests corroborated these findings, confirming that the new formula predicts drag increments more reliably.

Overall, while the application of vortex generators holds substantial promise for improving aircraft performance, further research is essential to overcome existing challenges and to harness their full potential more effectively. Future studies should focus on refining computational models, exploring the effects of VGs under a broader range of operational conditions, and addressing practical deployment issues to ensure the reliable and efficient integration of VGs in aircraft design.

In an effort to optimize aerodynamic efficiency and reduce drag, Lewthwaite and Amaechi (2022) conducted a comprehensive analysis of two wing modifications aimed at drag reduction: the addition of winglets to fighter aircraft and the implementation of dimpled surfaces on NACA 0017 aerofoils. By utilizing two commercial Computational Fluid Dynamics (CFD) platforms, the study explored novel solutions to optimize aircraft performance. The results demonstrate significant enhancements in lift and reductions in drag, affirming the effectiveness of these aerodynamic modifications.

Further advancing the field of flow separation control, Ciobaca et al. (2013) investigated active flow separation control as a means to enhance the lift of wing bodies under low-speed conditions. Their study employed computational simulations to evaluate the effectiveness of pulsed blowing at moderate momentum on the trailing edge flap. The researchers utilized both steady and unsteady Reynolds Averaged Navier-Stokes (RANS) approaches. Their findings demonstrate that constant blowing rates were effectively computed using steady RANS, while the unsteady RANS approach was instrumental in confirming the feasibility of active flow control even when high computational resources were required.

Asli et al. (2015) explored a novel passive stall control mechanism inspired by the leading edge protuberances observed on the flippers of humpback whales. This investigation focused on the thick airfoil S809, where aerodynamic coefficients at various static angles of attack were validated against the experimental data published by Somers in an NREL report. The study employed a computational fluid dynamics (CFD) approach at a Reynolds number of 10^6. Subsequent redesigns of the airfoil featured sinusoidal wavy leading edges. Computational results indicated that, compared to the baseline model, the modified airfoil configurations exhibited a marginal decrease in the lift coefficient at low angles of attack, prior to reaching the stall region.

In a related study, Livya et al. (2015) investigated the impact of the dimple effect on delaying the flow separation point at stall and reducing drag on aircraft wings. The aim was to enhance the agility of the aircraft. Utilizing the NACA 0018 airfoil, their research involved both theoretical and experimental analyses under varied angles of attack (5, 10, 15, 20, and 25 degrees) with inlet velocities of 30 and 60 m/s. Different dimple shapes semi-sphere, hexagon, cylinder, and square were examined. Their findings corroborate that the dimple effect improves the lift-to-drag (*L/D*) ratio, thereby significantly boosting aerodynamic efficiency and overall aircraft performance.

This survey shows that the study of flow separation on airfoils is a dynamic field that combines theoretical, experimental, and applied research. It remains a critical area in aerodynamics, particularly in improving the performance, safety, and efficiency of aircraft. The collective research reviewed investigates the use of vortex generators (VGs) and other aerodynamic modifications like dimples to enhance aircraft performance. Although drag reduction devices such as vortex generators (VGs) and dimpled surfaces are effective in reducing overall drag force to a degree, their impact on stability and the turbulence they create post-application do not significantly enhance overall aircraft performance. This limitation often restricts the use of such drag reduction devices in aircraft design. Furthermore, most researchers focus predominantly on reducing drag, yet they frequently overlook the importance of increasing lift and improving stability. Therefore, it is crucial to develop drag reduction techniques that not only achieve a higher *L/D* ratio but also

enhance stability, thereby improving overall aircraft performance.

This study was driven by the need to numerically assess *L/D* ratio for enhanced performance through the implementation of a boundary layer device, compared to a base model, as well as to evaluate the effects on flow behavior in both cases. To achieve these objectives, we introduced a technique known as the 'Rotating Thin Wire Method' to delay flow separation. Numerical simulations were used to examine the coefficient of drag (C_D), coefficient of lift (C_L), and C_L/C_D at various angles of attack for both scenarios with and without the device. We also compared the velocity contours for the base model in scenarios with and without the device. Additionally, pressure and turbulence intensity were measured for the models featuring the device on the wing model. The analysis concluded that the device effectively increased the coefficient of lift, reduced the coefficient of drag, and improved the overall performance of the aircraft.

2. DESIGN AND METHODOLOGY

The research's initial phase begins with collection of literature review. The study of the literature is based on the effective delay of flow separation. The literature consists of various aerodynamic devices and its characteristics. Pre-processing in ANSYS Fluent refers to the steps taken before the actual simulation process begins. This phase is critical because it determines the quality and accuracy of the simulation results. The design parameters are chosen for the modelling of the aircraft wing based on the literature survey. In order to delay the flow separation and decrease the drag, we studied and implemented the thin wire as aerodynamic device at different angle of attack. In the design process.

Aircraft wing design is a critical aspect of aircraft design, as the wing is responsible for generating the lift required to keep the aircraft aloft. The design of an aircraft wing is a complex process that involves considerations of aerodynamics, structural design, materials science, and manufacturing. This paper is mainly focused on the aerodynamics of aircraft wing. The design of the airfoil is critical to the performance of the wing, as it determines the lift and drag characteristics of the wing. The shape of the airfoil is typically analysed using XFLR software to determine the coefficient of lift, coefficient of drag and C_L/C_D at various angle of attack.

2.1 Airfoil Selection

An airfoil is a specially designed shape of a wing, blade, or any other structure that is designed to generate lift as it moves through the air. Airfoils are an essential part of the design of aircraft, wind turbines, and other machines that move through air. The shape of an airfoil is carefully designed to create a pressure difference between the upper and lower surfaces, which generates lift. From the problem statement we have selected NACA 63418 as root chord airfoil and NACA 63415 as tip chord airfoil (Grasso, 2010).

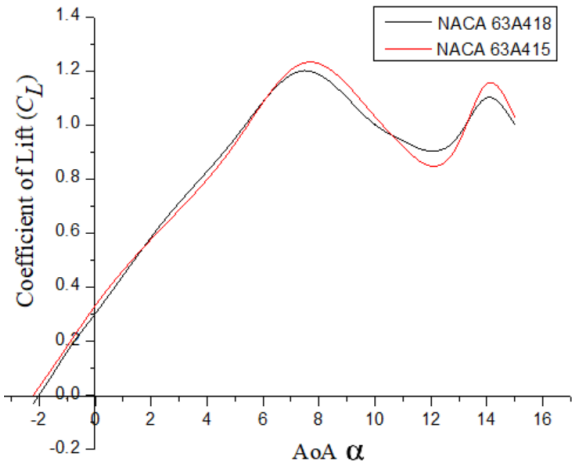

Fig. 1 C_L vs alpha (Grasso, 2010)

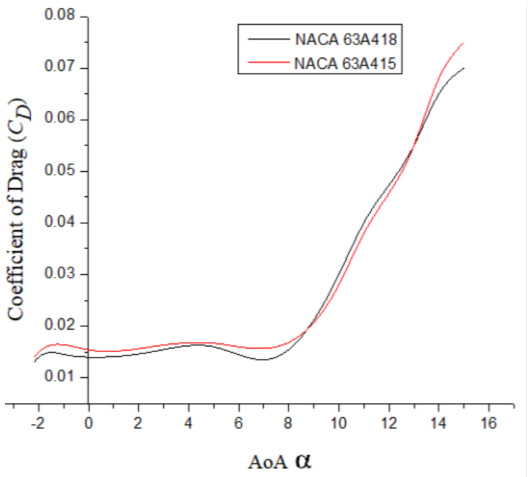

Fig. 2 Cd vs alpha (Grasso, 2010)

Figure 1 represents the C_L vs α graph and it is a plot that shows the variation of the lift coefficient (C_L) with α for above mentioned airfoil. The C_L vs α graph typically shows a nonlinear relationship between C_L and α, with C_L increasing rapidly at low angles of attack and reaching a maximum value at a particular angle of attack, called the maximum lift coefficient (C_{Lmax}). The α at which C_{Lmax} occurs between 8 to 10 degrees for our airfoil. As the α is increased beyond C_{Lmax}, the lift coefficient decreases rapidly, and eventually reaches a point where the airfoil stalls, resulting in a sudden drop in lift. The α at which stall occurs is called the stall angle, and in our case the stall is between 10 to 15 degrees. The Fig. 2 represents the C_D vs α graph and it is a plot that shows the variation of the drag coefficient (C_D) with α for above mentioned airfoil. The C_D vs α graph typically shows a nonlinear relationship between Cd and alpha, with C_D initially increasing slowly at low angles of attack and then increasing more rapidly as the α is increased. This increase in C_D is due to the increase in skin friction drag and pressure drag as the flow around the airfoil becomes more turbulent. This graph can provide useful information about the drag characteristics of an airfoil, including its drag coefficient at different angles of

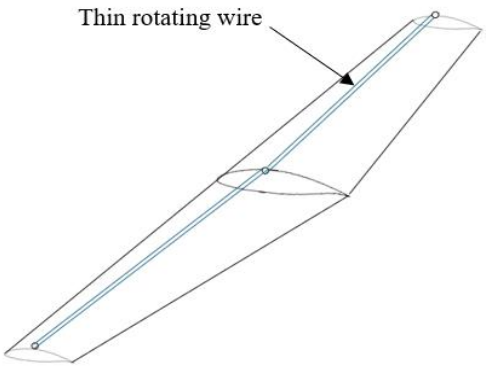

Fig. 3 Schematic of wing geometry with thin wire attachment

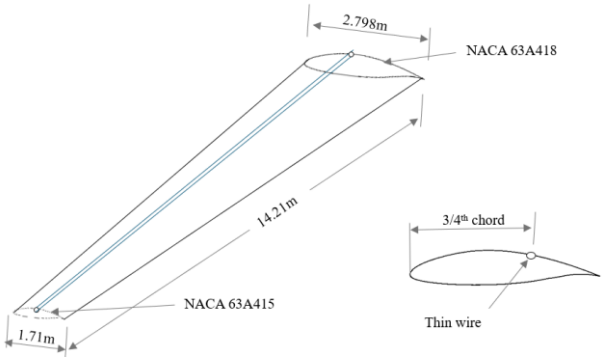

Fig. 4 Schematic of wing and its specifications

Table 1 Wing specifications

Wing root chord airfoil	NACA 63A418
Wing tip chord airfoil	NACA 63A415
Wing span	28.42 m
Wing root chord	2.798 m
Wing tip chord	1.710 m
Wing area	64 m^2
Aspect ratio	12.6
Thickness of thin wire	50 mm

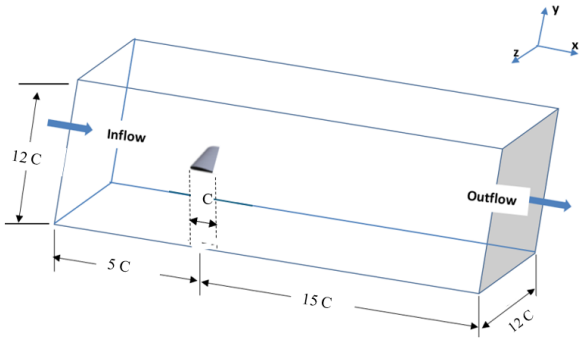

Fig. 5 Computational domain

attack, the α at which the airfoil produces the minimum drag, and the onset of flow separation and turbulence.

2.2 Wing Specifications & Thin Wire

The geometry of an aircraft wing is an important aspect of its design, as it determines the wing's aerodynamic characteristics and structural properties. The main geometric features of an aircraft wing include wing span, wing area, wing aspect ratio, wing taper and wing thickness (Panigrahi et al., 2021).

These geometric features are carefully considered and optimized during the wing design process to ensure that the wing provides the necessary lift and performance characteristics for the aircraft. The use of advanced computer-aided design tools, such as CATIA V5 and analysis tools such as computational fluid dynamics (CFD) allows designers to model and optimize the geometry of the wing for maximum performance and efficiency. The Fig. 3 represent the geometry of the wing with thin wire and Table 1 represent the wing specification.

Figure 4 represent the wing with implementation of thin wire at 3/4th of the chord length and Table. 1 represent the specification of wing geometry with thin wire.

3. COMPUTATIONAL ANALYSIS

CFD (Computational Fluid Dynamics) analysis is a powerful tool used in a wide range of engineering fields to simulate and analyse the behaviour of fluids in complex systems. CFD analysis is important because it allows engineers to predict and optimize the performance of systems before they are built, reducing the need for costly and time-consuming physical testing.

3.1 Computational Domain

Domain creation is an essential step in airfoil analysis because it defines the computational region where the fluid flow is analyzed. The domain includes the airfoil geometry, the surrounding fluid region, and the boundaries that define the flow domain. The proper domain creation is essential to accurately define the domain to ensure accurate and reliable results. Proper domain definition helps in generating a high-quality mesh, efficient utilization of computational resources, and accurate modelling of the flow physics. The domain specification is described in Fig. 5.

3.2 Meshing

The meshing is the process of dividing the geometry into a collection of small elements or cells. Meshing is an essential step in computational fluid dynamics (CFD) simulations because it directly affects the accuracy and computational efficiency of the analysis. ANSYS Fluent supports various meshing techniques, including structured, unstructured, hybrid, and adaptive meshing. Structured meshes have regular shapes and are typically used for simple geometries, while unstructured meshes have irregular shapes and are useful for complex geometries. In our analysis we used unstructured meshes to determine the result. The element quality refers to the measure of the distortion or irregularity of the elements in a mesh. Elements that are distorted or have irregular shapes can lead to inaccurate numerical results and can

Table 2 Fine Mesh

Element size	50 mm			
Node	885701			
Element	4885010			
Fine Mesh – Quality Criteria				
Quality criteria		**Min**	**Max**	**Average**
Element Quality		6.74E-08	0.99914	0.79234
Skewness	Skewness<0.8	0.0011609	0.92977	0.23539
Orthogonality	0.5 < ortho >0.7	2.16E-07	0.99107	0.72873

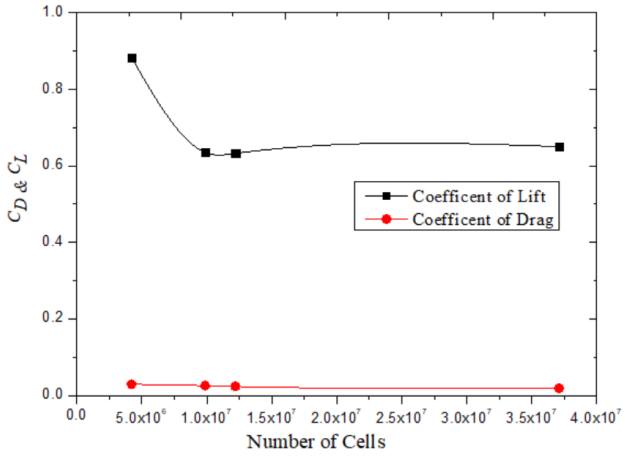

Fig. 6 C_D & C_L trend for GIS

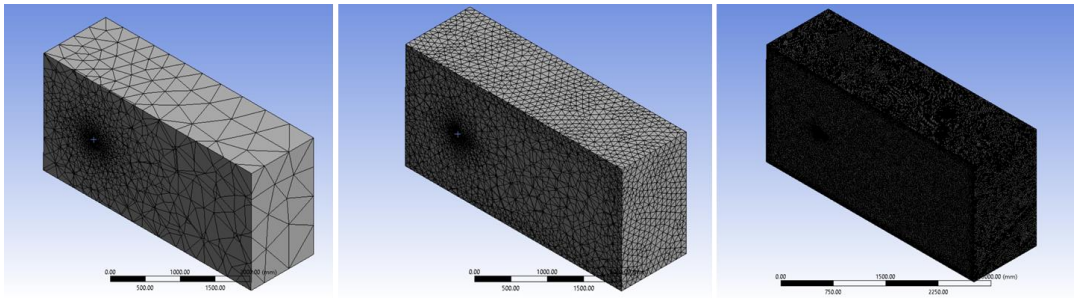

Fig. 7 Base mesh, Coarse mesh and Fine mesh

cause convergence problems during simulation. There are different measures of element quality in ANSYS Fluent, including aspect ratio, skewness, and orthogonality. The aspect ratio measures the ratio of the longest to the shortest side of an element, while skewness measures the deviation of an element from a perfectly equilateral shape. Orthogonality measures the angle between the faces of an element. It is important to ensure that the mesh used in ANSYS Fluent has good element quality to obtain accurate and reliable results (Shahzad et al., 2019).

3.3 Grid Independence Study (GIS)

Grid independence study is an important step in computational fluid dynamics (CFD) simulations, which involves examining the sensitivity of the numerical results to changes in the grid size or resolution. It is essential to perform a grid independence study to ensure that the simulation results are accurate and reliable, and do not depend significantly on the mesh size.

Four different mesh sizes 4.21×10^6, 9.87×10^6, 1.22×10^7, and 3.71×10^7 cells, labeled Mesh 1, Mesh 2, Mesh 3, and Mesh 4, respectively were evaluated in a grid independence test to select the optimal mesh size for the numerical study. This range facilitated progression from a coarse to a fine mesh. Lift and drag, the primary focus parameters, were assessed by comparing the coefficients of drag across these meshes, with the results depicted in Fig. 6. The Grid Independence Study revealed that refining the mesh from Mesh 1 to Mesh 4 led to reductions of approximately 11% in C_L and 4% in C_D. Despite differing cell counts, both Mesh 3 and Mesh 4 exhibited identical C_L values of about 0.63 and C_D values of approximately 0.023. Therefore, to minimize computational time, the coarser Mesh 3, which contains 12,234,182 cells, was selected for the numerical analyses.

The Fine mesh specification and quality criteria is discussed in Table 2 and Fig. 7 represent the mesh metrics of Fine mesh.

Table 3 Inflation layer specifications

Velocity	180 m/s
Length scale	0.50374
Viscosity	1.81e-5 pa-s
Target (y+)	1
Inflation layer	30
Inflation Layers	4.30e-06
Growth rate	1.2

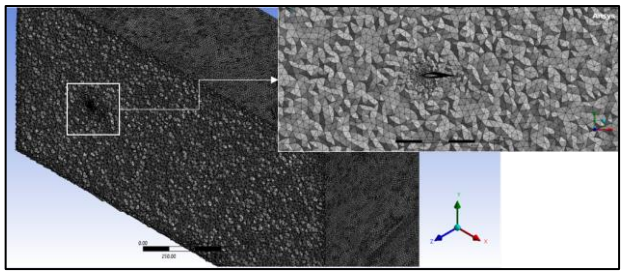

Fig. 8 Volumetric mesh

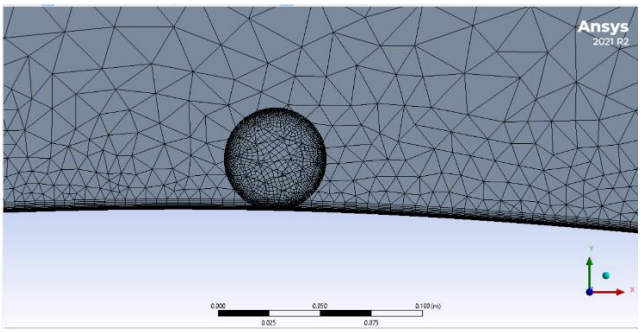

Fig. 9 Mesh of rotating domain

A volumetric mesh is a type of mesh used in ANSYS Fluent that is composed of a three-dimensional grid of cells or elements. This type of mesh is used to discretize the three-dimensional domain of a fluid flow problems. The Figs. 8 & 9 represent the volumetric mesh and the mesh of the rotating domain, respectively.

An inflation layer is a special type of mesh layer that is used to accurately capture the boundary layer of a fluid flow as shown in Fig. 10 and Table 3. The boundary layer is the thin layer of fluid that exists next to a solid surface in which the velocity and other fluid properties are affected by the presence of the surface. Inflation layers are typically used in problems where the flow near a solid boundary is of interest, such as in the simulation of aerodynamic flows over aircraft wings. The purpose of the inflation layer is to increase the resolution of the mesh near the boundary to accurately capture the flow physics and prevent numerical errors (Supreeth et al., 2020).

To calculate the height of the first cell layer for an inflation layer, h = y+*(delta) where, h is the height of the first layer, y+ is the desired target value of the y+ parameter, delta is the distance from the wall to the first cell centre. The y+ parameter is a dimensionless parameter that describes the distance of the first cell centre from the wall in units of the molecular viscosity length scale. The distance delta can be calculated using delta = k * d, where d is the size of the first cell adjacent to the wall, and k is a

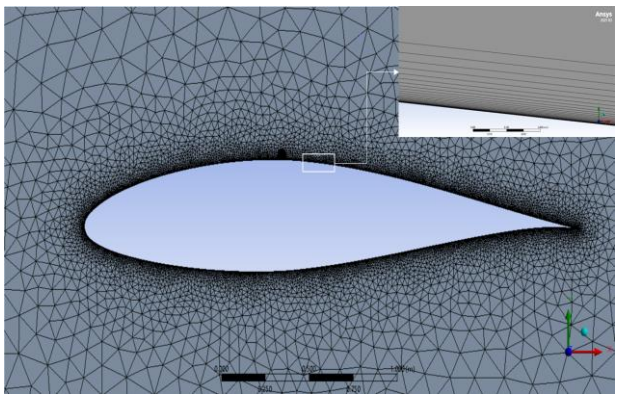

Fig. 10 Inflation layer

constant that depends on the type of wall function used in the simulation.

The purpose of the setup in ANSYS Fluent is to prepare the simulation environment for the fluid flow analysis. It involves boundary conditions, solver settings, and post-processing options for the simulation. The setup process is a critical step in any CFD analysis, as it directly affects the accuracy and reliability of the simulation results. A well-defined setup ensures that the simulation accurately captures the physical behaviour of the fluid flow and provides meaningful insights into the system being studied. The boundary conditions that govern the flow behaviour at the boundaries of the simulation domain. This involves specifying the inlet and outlet conditions, wall conditions, and any other relevant boundary conditions. After the boundary conditions are defined, the solver settings need to be specified. This includes selecting an appropriate solver method, specifying the convergence criteria, and defining any other relevant solver settings.

The pressure-based solver type is chosen because it is a incompressible flow where density is kept constant. The steady-state simulations are often used when the flow variables have reached a state of equilibrium and the time-varying behaviour of the flow is no longer important. The k-epsilon model is designed to accurately predict turbulence in a wide range of flow conditions, including both laminar and turbulent flows (Table 4). It is based on the Reynolds-averaged Navier-Stokes (RANS) equations and provides a balance between accuracy and computational efficiency. The k-epsilon model can handle complex flows with features such as swirl, recirculation, and separation.

Table 4 Solver setup

Solver type	Pressure based
Solver time	Transient
Model	Viscous(Realizable) k-epsilon
Rotational velocity	900 Rpm
Inlet velocity	180 m/s
Density (ρ)	1.225 kg/m3
Viscosity (μ)	1.7892 x 10-5 Kg/ms-1
Operating Pressure (P)	1.01325 bar
Wall	No slip condition

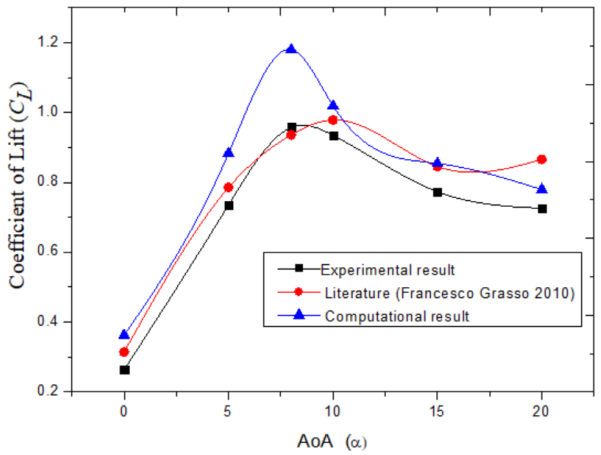

Fig. 11 C_L vs α

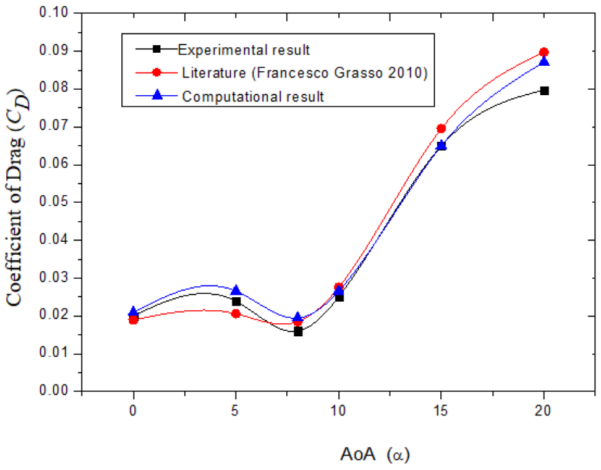

Fig. 12 C_D vs α

Typically, post-processing technology that is connected to pre-processing and simulation software is used to show the outcomes of CFD. In the post-processing process, the contour and the lift, drag, coefficient of drag, and coefficient of lift produced by the wing with and without implementation of thin wire are obtained. These results are compared and discussed in result and analysis.

4. RESULT AND ANALYSIS

This section delves into the results and subsequent analysis of our simulation studies. It illustrates the use of advanced graphical techniques, including contour plots, vector plots, and streamlines, to represent the flow variables comprehensively. By leveraging these visual tools, we aim to highlight the critical features and dynamics of the fluid flow within the system under investigation. The discussion will also emphasize the pivotal role of post-processing in ANSYS Fluent simulations. This process is instrumental in enabling engineers and researchers to extract and interpret valuable information from the data, thereby enhancing their understanding of the fluid flow's behavior. The insights gained from these analyses are vital for both theoretical advancements and practical applications in fluid dynamics.

The Fig. 11 represents the C_L vs α for wing without aerodynamic device implementation. The C_L vs α graph shows the rapidly increasing C_L at low angles of attack and reaching a maximum value at a particular α (C_{Lmax}). The α at which C_{Lmax} occurs between 7 to 9 degrees for wing without implementation of thin wire. The coefficient of lift eventually reaches a point where the airfoil stalls, resulting in a sudden drop in lift. The α at which stall occurs is called the stall angle, and in our case the stall is between 10 to 15 degrees. The Fig. 12 represents the C_D vs α for wing without aerodynamic device implementation.

The Fig. 12 C_D vs α graph typically shows a nonlinear relationship between C_D and α, with C_D initially increasing slowly at low angles of attack and then increasing more rapidly as the α is increased. This increase in C_D is due to the increase in skin friction drag and pressure drag as the flow around the airfoil becomes more turbulent. The

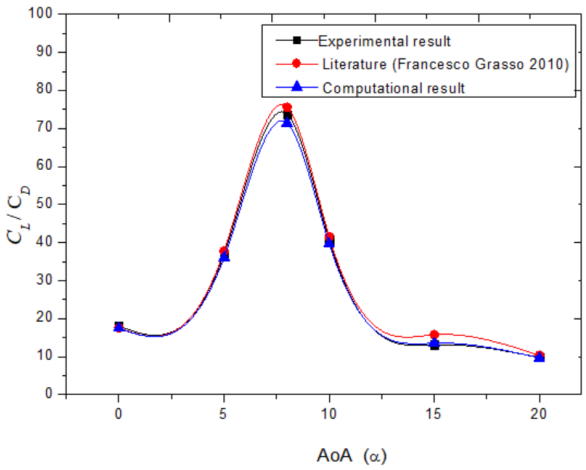

Fig. 13 C_L/C_D vs α

creation of maximum drag leads to the onset of flow separation and turbulence. The below Fig. 13 represents the C_L/C_D vs α for wing without aerodynamic device implementation.

Figure 13 C_L/C_D vs α graph, also known as the lift-to-drag polar graph, shows the ratio of lift coefficient to drag coefficient as a function of the α of an airfoil. The cl/cd vs alpha graph is used to study the aerodynamic performance of an airfoil, which is an important factor in the design of aircraft. The cl/cd vs alpha graph typically shows a parabolic curve that peaks at a certain angle of attack, known as the angle of maximum lift-to-drag ratio or *L/D* max. This angle represents the optimal α for the airfoil, where the lift generated is maximum for a given amount of drag. At angles of attack higher or lower than the angle of *L/D* max, the ratio of lift to drag decreases due to the increasing drag or decreasing lift generated by the airfoil. The table 6.1 represents the C_L, C_D and C_L/C_D produced at various α for wing without implementation if aerodynamic devices.

In order to validate the computational results, a comparative study was conducted using both existing computational and experimental results, alongside the literature from Francesco Grasso (2010). The referenced

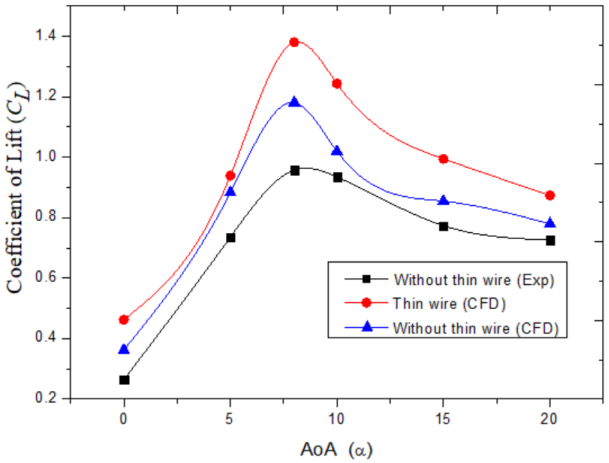

Fig. 14 C_L *vs* α

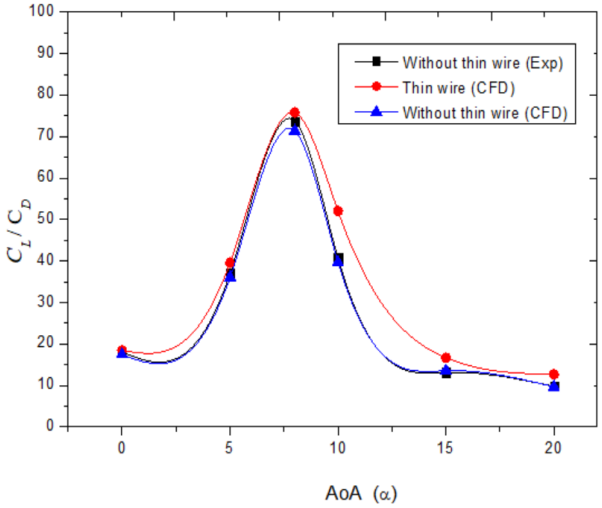

Fig. 16 C_L/C_D vs α

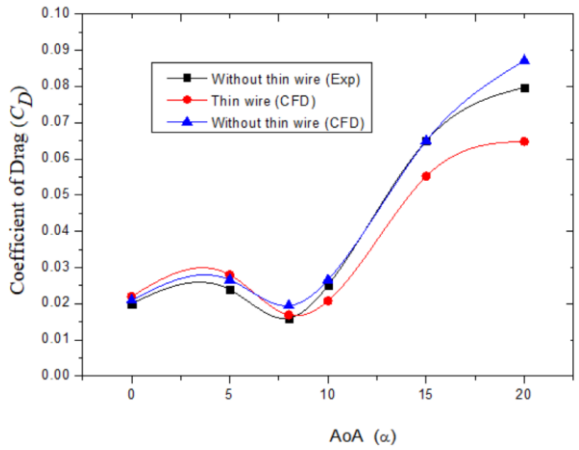

Fig. 15 C_D vs α

experimental results were derived from an open circuit subsonic wind tunnel, set up to simulate real flying conditions for a scaled wing model without the use of thin wire. The coefficients of drag (C_D) and lift (C_L), as well as the ratio of C_L to C_D (C_L/C_D) for the wing model without thin wire at various angles of attack, were obtained from the numerical studies of the current research, experimental results (Lakshmanan et al., 2023), and literature, and are presented in Figs 11 to 13. Notably, only minor variations in C_L, C_D & (C_L/C_D) with α were observed for all the cases.

4.1 Implementation of Thin Wire

The Fig. 14. represents the C_L vs α for wing with aerodynamic device implementation. The α which C_{Lmax} occurs at 15 degree α for wing with implementation of thin wire. The coefficient of lift eventually reaches a point where the airfoil stalls, resulting in a sudden drop in lift. The α at which stall occurs is called the stall angle, and in our case the stall starts above 15 degree angle of attack.

The Fig. 15 represents the C_D vs α for wing with aerodynamic device implementation. The C_D vs α graph typically shows a nonlinear relationship between C_D and α alpha, with C_D initially increasing slowly at low angles of attack and then increasing more rapidly as the α is increased. In our case when the thin with is rotated with certain rpm the C_D increases slowly from 0 degree α and drop from 6 to 10 degree and rapidly increases when there is increase in angle of attack.

The Fig. 16 represents the C_L/C_D vs α for wing with aerodynamic device implementation. The C_L/C_D vs α graph typically shows a parabolic curve that peaks at a certain angle of attack, known as the angle of maximum lift-to-drag ratio or *L/D* max. This angle represents the optimal α for the airfoil, where the lift generated is maximum for a given amount of drag. In our case the max C_L/C_D is at 10^o α.

A velocity contour is a graphical representation of the velocity field within a fluid domain. It displays the velocity magnitude and direction at each point in the domain using color-coded or contour lines. The velocity contour plot can be used to visualize and analyse the fluid flow behaviour in the domain. By examining the contour plot, we can identify regions of high and low velocity, areas of flow separation, and regions of recirculation. The below Fig. 17. represents the velocity contour of the wing at various angle of attack. In the Fig. 17 the red colour represents the high velocity region and blue colour represents the low velocity region.

The pressure contour plots provide a useful tool for visualizing and analysing the pressure behaviour in a domain, and for understanding the complex interactions between the fluid and the surrounding structures. The Fig. 18 represents the pressure contour of the wing at various angle of attack and presents, the pressure on the upper surface decreases significantly due to the faster airflow, creating a low-pressure region that contributes to lift. This is contrasted by a higher pressure region on the lower surface.

The TKE contour plot can be used to visualize and analyse the intensity of the turbulent motion within the flow domain. By examining the contour plot, we can identify regions of high and low TKE, and gain insights into the behaviour of the turbulence within the domain. The below Fig. 19 represents the turbulent kinetic energy contour of the wing at various angle of attack.

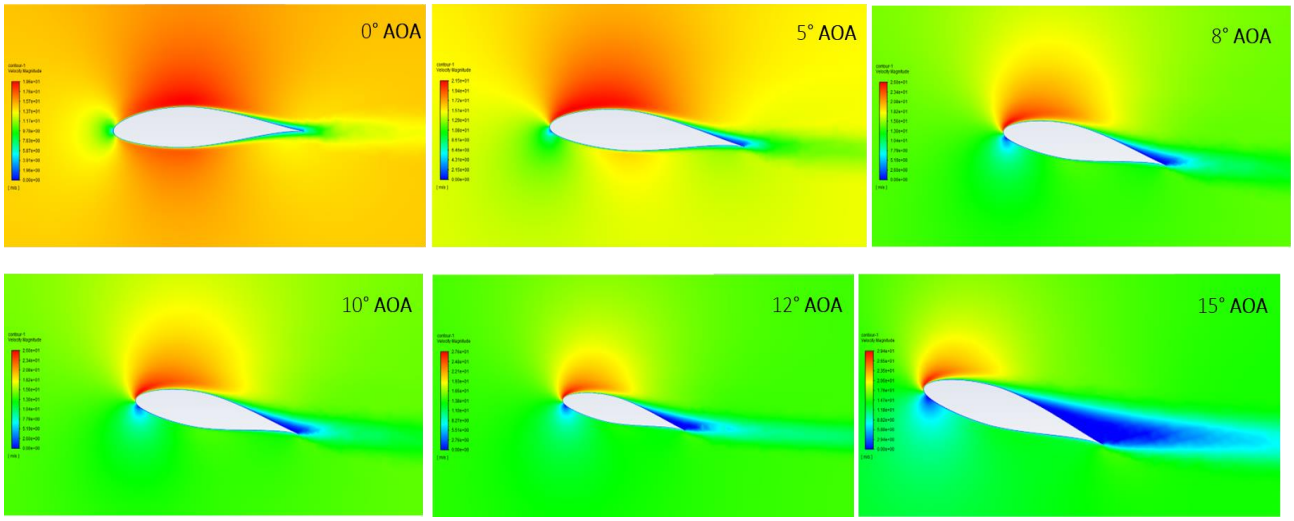

Fig. 17 Flow field variation at various AOA (0º, 5º, 8º, 10º, 12º, 15º) of base model

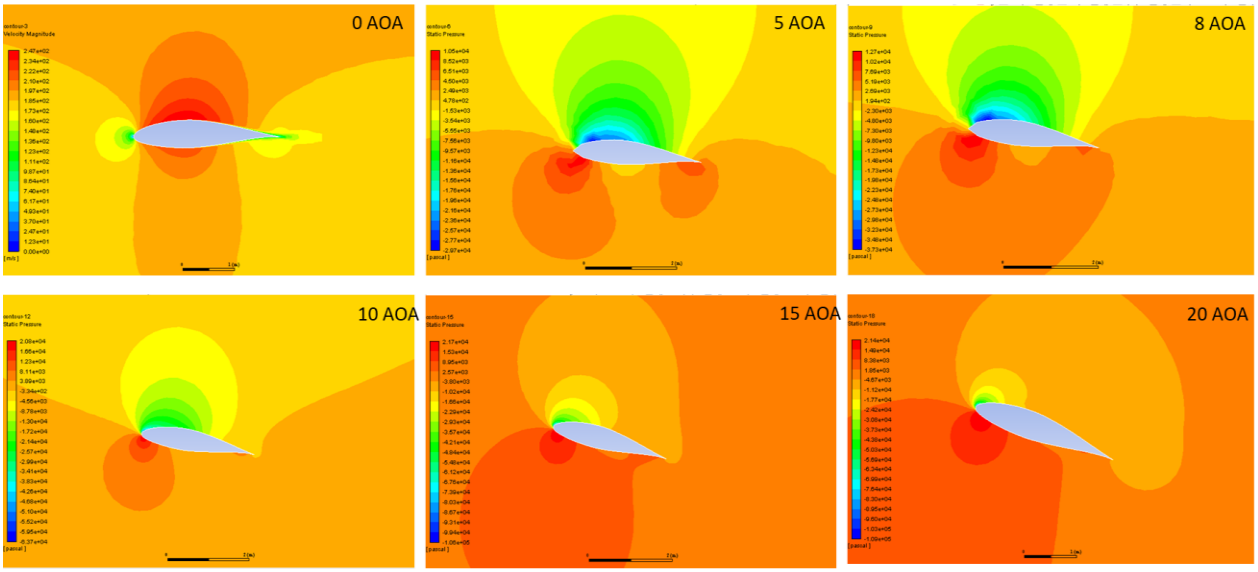

Fig. 18 Pressure variation at various AOA (0º, 5º, 8º, 10º, 15º, 20º) of base model

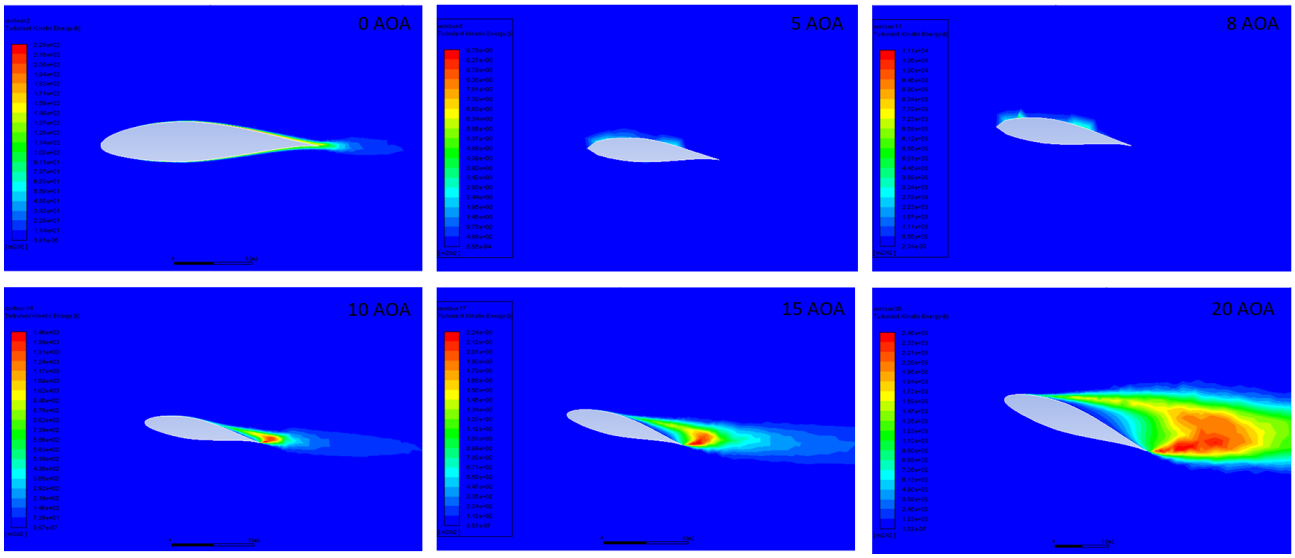

Fig. 19 Turbulence intensity variation at various AOA (0º, 5º, 8º, 10º, 15º, 20º) of base model

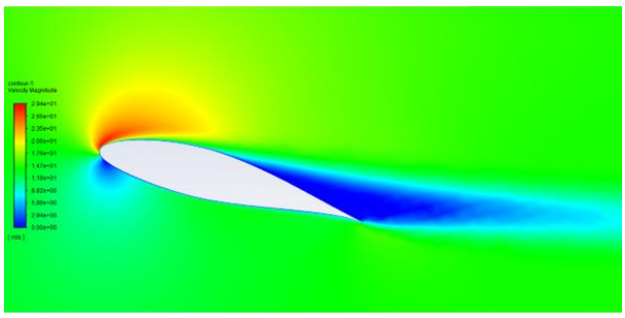

Fig. 20 Velocity contour for without thin wire

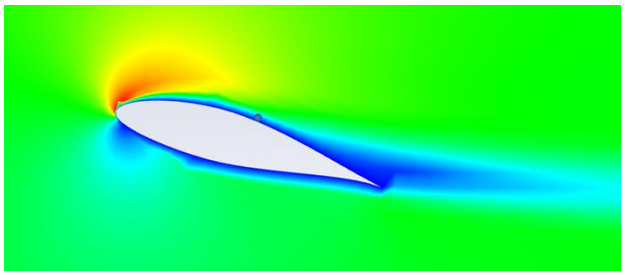

Fig. 21 Velocity contour for thin wire without rotation

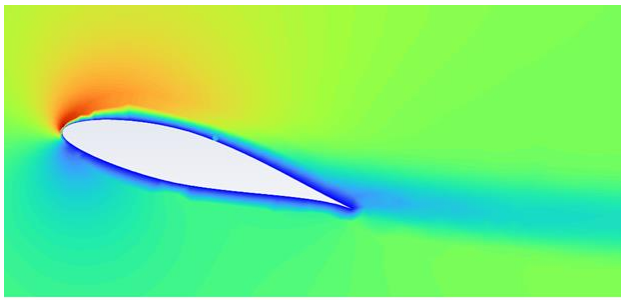

Fig. 22 Velocity contour for thin wire with rotation

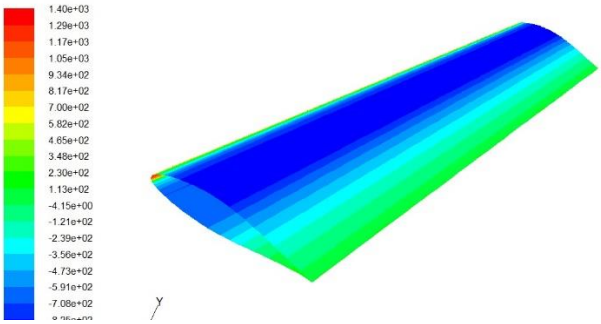

Fig. 23 Pressure contour for without thin wire

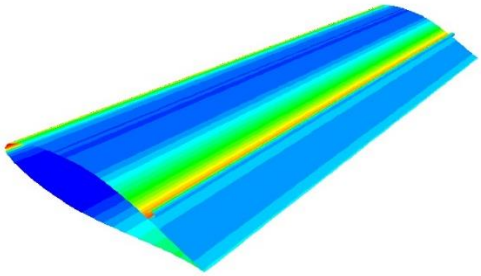

Fig. 24 Pressure contour for thin wire without rotation

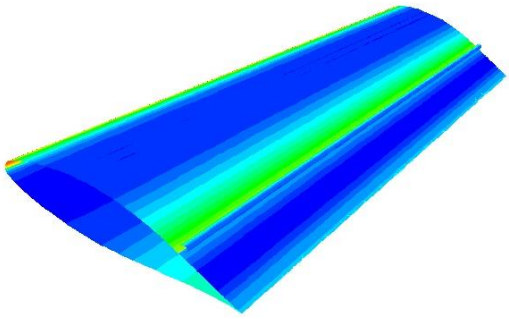

Fig. 25 Pressure contour for thin wire with rotation

4.2 Comparison of Flow Behaviour

Figure 20 to 21 represents the velocity contour of both the cases. This contour represents the attachment of flow over the surface. Here it is observed that at 15-degree and 20-degree α the flow separates at 50% and 30% respectively. But when we implemented the rotating thin wire at 50% of the chord, we can delay the flow separation. Hence, we achieved the reduction of stall at high angle of attack.

Computational analysis of pressure distribution over wing provides a comprehensive view of the aerodynamic forces at play. This analysis begins with the creation of a detailed 3D model of the wing, incorporating its geometric characteristics. The model is then subjected to airflow simulations under various conditions, such as with and without thin wire and rotation of wire. During the simulation, the airflow around the wing is resolved into a grid or mesh, where the Navier-Stokes equations are numerically solved to capture the behavior of the fluid. The resulting pressure contours highlight how pressure varies over the wing surface. Figure 23 to 25 represents, the pressure on the upper surface decreases significantly due to the faster airflow, creating a low-pressure region that contributes to lift. This is contrasted by a higher pressure region on the lower surface.

Key areas examined in these simulations include the leading edge, where the pressure peaks due to the impact of incoming air, and the trailing edge, where complex flow phenomena such as vortices and potential flow separation can occur. These simulations can reveal regions of high pressure near the leading edge that gradually decrease along the chord to the trailing edge on the upper surface. Conversely, the lower surface often shows a more gradual pressure increase towards the trailing edge compared to higher for wing with rotation of thin wire (Figs. 22 & 25) than others conditions (Figs 23 & 24).

Improving the streamlines over wing based on CFD results involves analyzing the flow patterns and pressure distributions to identify areas of adverse airflow characteristics such as turbulence, flow separation, or excessive drag. The thin wire with rotation method to enhance streamlining is by refining the streamline pattern, particularly the leading and trailing edges and delay flow separation and early attaching the flow after the thin wire

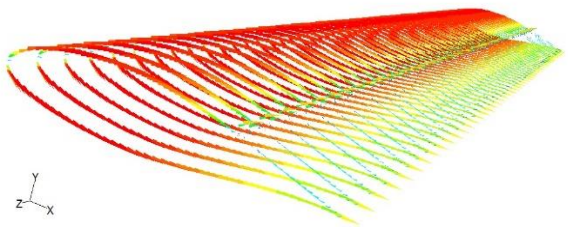

Fig. 26 Streamline pattern for without thin wire

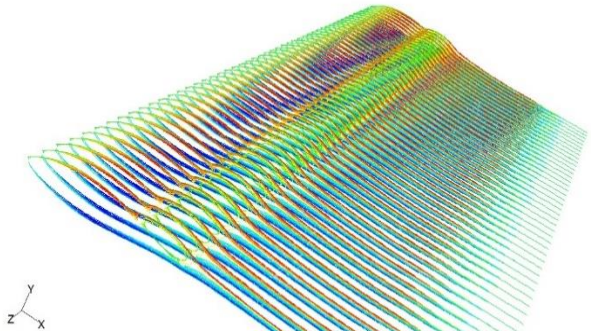

Fig. 27 Streamline pattern for thin wire without rotation

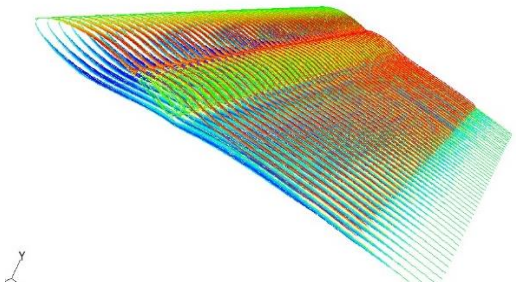

Fig. 28 Streamline pattern for thin wire with rotation

placed shown in Fig. 28. This modified to have a more gradual curvature, reducing the pressure peak and allowing for smoother airflow over the wing.

This approach is maintaining laminar flow over a larger portion of the wing, drag can be significantly reduced. This can be achieved through magnus effect of rotation of thin wire. Adjusting these parameters can improve the alignment of streamlines with the wing surface, reducing flow separation and enhancing overall aerodynamic efficiency. Deploying thin wire, placed on the wing, can also help in re-energizing the boundary layer, delaying flow separation and maintaining smoother airflow over the wing compared to without thin wire model and without rotation as shown in Fig. 26 & 27.

Incorporating these improvements based on detailed CFD analysis ensures that the wing design promotes optimal airflow characteristics, reduces drag, and enhances lift, leading to better fuel efficiency and performance. This thin wire modifications, guided by high-fidelity CFD simulations, allow engineers to fine-tune the aerodynamic properties of the wing, achieving a more streamlined and efficient aircraft.

Figure 14 illustrates the comparative analysis of the coefficient of lift (C_L) for cases with and without the implementation of thin wire. In the graph, the blue line denotes C_L without the implementation of thin wire, while the red line represents C_L achieved when the thin wire is rotated at 900 rpm. From 0 to 8 degrees angle of attack, C_L increases significantly upon the introduction of thin wire; beyond this, at stall angles such as 10, 15, and 20 degrees, C_L reaches its maximum compared to the case without thin wire implementation. Specifically, there is a 28.47% increase in C_L at a 15^o α when thin wire is implemented.

Figure 15 depicts the comparison of the coefficient of drag (C_D) for both scenarios with and without thin wire implementation. The graph indicates that from 0 to 8 degrees angle of attack, the drag increases with the rotation of thin wire. However, beyond 8 degrees, a decrease in drag is observed, aligning with our objective to reduce drag in cases of flow detachment. Notably, C_D decreased by 15.07% at a 15^o α with thin wire implementation.

Moreover, Fig. 16 provides a comparative graph of the ratio of the coefficient of lift to the coefficient of drag (C_L/C_D) for both implementation scenarios. The data reveal that C_L/C_D decreases from 0 to 8 degrees angle of attack, but increases at stall angles such as 10, 15, and 20 degrees, indicating improved performance. The implementation of thin wire resulted in a 26.81% increase in C_L/C_D at a 15^o α. Consequently, by delaying flow separation, we achieved enhanced aerodynamic performance, thereby addressing the initial problem statement aimed at reducing drag in conditions of flow separation.

5. CONCLUSION

In summary, this research successfully explores the optimization of the lift-to-drag (L/D) ratio through strategic modifications to wing geometry and the incorporation of aerodynamic devices, particularly focusing on the deployment of a rotating thin wire. Through comprehensive analyses conducted at various angles of attack, ranging from 0 to 20 degrees, we demonstrated that the introduction of rotational elements at specific points along the wing chord significantly delays the onset of flow separation and stall.

Notably, our findings, the velocity contours confirmed that flow attachment was maintained up to higher angles of attack 15 ^{o} and 20 ^{o} particularly when the thin wire was implemented. This intervention led to a substantial increase in the coefficient of lift (C_L), with a peak increase of 28.47% at a 15^o angle of attack. Furthermore, the implementation of the thin wire not only elevated the C_L but also effectively reduced the coefficient of drag C_D by 15.07% at the same angle, directly contributing to our goal of minimizing drag under conditions of flow detachment. Additionally, the ratio of lift to drag (C_L/C_D) showed significant improvements, particularly in stall conditions, with an increase of 26.81% at a 15^o angle of attack. These enhancements affirm the

potential of integrating rotational elements into the wing's aerodynamic design to elevate overall aircraft performance by optimizing the *L/D* ratio and extending the operational envelope through delayed flow separation and reduced stall propensity.

Ultimately, this study contributes valuable insights into the design and implementation of passive aerodynamic devices aimed at improving the efficiency and performance of aircraft wings under various flight conditions. The outcomes not only support the theoretical underpinnings of flow dynamics but also offer practical pathways for future aerodynamic research and development in aviation technology.

ACKNOWLEDGMENTS

The author acknowledges the assistance provided by SRM Valliammai Engineering College throughout the computational analysis as well as the direction provided by the research park R&D at the Bannari Amman Institute of Technology in order to accomplish this research.

CONFLICT OF INTEREST

The authors have no conflict of interest to disclose in this research work.

AUTHORS CONTRIBUTION

J P Ramesh: Developed conceptualization, methodology, validation and Writing; **V Mugendiran:** Performed writing - Oral draft preparation, reviewing; **G Sivaraj:** Performed - Designing, reviewing and editing.

REFERENCES

Anand, U., Sudhakar, Y., Thileepanragu, R., Gopinathan, V. T. & Rajasekar, R. (2010, December 16-18). Passive flow control over NACA0012 aerofoil using vortex generators. *the 37th International & 4th National Conference on Fluid Mechanics and Fluid Power*, IIT Madras, Chennai, India. https://www.researchgate.net/publication/320935360_PASSIVE_FLOW_CONTROL_OVER_NACA0012_AEROFOIL_USING_VORTEX_GENERATORS

Asli, M., Mashhadi Gholamali, B., & Mesgarpour Tousi, A. (2015). Numerical analysis of wind turbine airfoil aerodynamic performance with leading edge bump. *Mathematical Problems in Engineering*, (2015). https://doi.org/10.1155/2015/493253

Ciobaca, V., Kühn, T., Rudnik, R., Bauer, M., Gölling, B., & Breitenstein, W. (2013). Active flow-separation control on a high-lift wing-body configuration. *Journal of Aircraft, 50*(1), 56-72. https://doi.org/10.2514/1.C031659

Grasso, F. (2010, July 28). Usage of Numerical Optimization in Wind Turbine Airfoil Design. *28th AIAA Applied Aerodynamics Conference*, Chicago, Illinois. https://publications.tno.nl/publication/34631245/r4M6e0/m10048.pdf

Ichikawa, Y., Koike, S., Ito, Y., Murayama, M., Nakakita, K., Yamamoto, K., & Kusunose, K. (2021). Size effects of vane-type rectangular vortex generators installed on high-lift swept-back wing flap on lift force and flow fields. *Experiments in Fluids, 62*, 1-17. https://doi.org/10.1007/s00348-021-03198-4

Ito, Y., Yamamoto, K., Kusunose, K., Koike, S., Nakakita, K., Murayama, M., & Tanaka, K. (2016). Effect of vortex generators on transonic swept wings. *Journal of Aircraft, 53*(6), 1890-1904. https://doi.org/10.2514/1.C033737

Kusunose, K., & Yu, N. J. (2003). Vortex generator installation drag on an airplane near its cruise condition. *Journal of Aircraft, 40*(6), 1145-1151. https://doi.org/10.2514/2.7203

Lakshmanan, D., Boopathi, R., & Saravanan, P. (2023). Aerodynamic investigation and simulation studies on wing section of an unmanned aerial vehicle attached with solar plate. *Journal of Applied Fluid Mechanics, 16*(8), 1666-1674. https://doi.org/10.47176/jafm.

Lewthwaite, M. T., & Amaechi, C. V. (2022). Numerical investigation of winglet aerodynamics and dimple effect of NACA 0017 airfoil for a freight aircraft. *Inventions, 7*(1), 31. https://doi.org/10.3390/inventions7010031

Mahboub, A., Bouzit, M., & Ghenaim, A. (2022). Effects of different shaped cavities and bumps on flow structure and wing performance. *Journal of Applied Fluid Mechanics, 15*(6), 1649-1660. https://doi.org/10.47176/jafm.15.06.1108

Manolesos, M., & Voutsinas, S. G. (2015). Experimental investigation of the flow past passive vortex generators on an airfoil experiencing three-dimensional separation. *Journal of Wind Engineering and Industrial Aerodynamics, 142*, 130-148. https://doi.org/10.1016/j.jweia.2015.03.020

Merryisha, S., & Rajendran, P. (2019). Experimental and CFD analysis of surface modifiers on aircraft wing: A review. *CFD Letters, 11*(10), 46-56. https://akademiabaru.com/submit/index.php/cfdl/article/view/3516

Namura, N., Shimoyama, K., Obayashi, S., Ito, Y., Koike, S., & Nakakita, K. (2019). Multipoint design optimization of vortex generators on transonic swept wings. *Journal of Aircraft, 56*(4), 1291-1302. https://doi.org/10.2514/1.C035148

Panigrahi, C., Chawla, R., & Nair, M. T. (2021). Optimisation of trapped vortex cavity for airfoil separation control. *Journal of Applied Fluid Mechanics, 15*(1), 179-191. https://doi.org/10.47176/jafm.15.01.32684

Saraf, A. A. K., Singh, B. M. P., & Chouhanr, C. T. S. (2018). Study of flow separation on airfoil with bump. *International Journal of Applied Engineering Research, 13*(16), 12868-12872. https://www.ripublication.com/ijaer18/ijaerv13n16_

67.pdf

Shahzad, A., Qadri, M. M., & Ahmad, S. (2019). Numerical analysis of high aspect ratio flexible wings in flapping motion. *Journal of Applied Fluid Mechanics*, *12*(6), 1979-1988. https://doi.org/10.29252/jafm.12.06.29792

Shan, H., Jiang, L., Liu, C., Love, M., & Maines, B. (2008). Numerical study of passive and active flow separation control over a NACA0012 airfoil. *Computers & Fluids*, *37*(8), 975-992. https://doi.org/10.1016/j.compfluid.2007.10.010

Supreeth, R., Arokkiaswamy, A., Anirudh, K., Pradyumna, R. K., Pramod, P. K., & Sanarahamat, A. K. (2020). Experimental and numerical investigation of the influence of leading edge tubercles on S823 airfoil behavior. *Journal of Applied Fluid Mechanics*, *13*(6), 1885-1899. https://doi.org/10.47176/jafm.13.06.31244

Wang, H., Zhang, B., Qiu, Q., & Xu, X. (2017). Flow control on the NREL S809 wind turbine airfoil using vortex generators. *Energy*, *118*, 1210-1221. https://doi.org/10.1016/j.energy.2016.11.003

Wik, E., & Shaw, S. (2004, June). *Numerical simulation of micro vortex generators.* 2nd AIAA Flow Control Conference (p. 2697). https://doi.org/10.2514/6.2004-2697

Yangwei, Z., Longfeng, H. & Diangui, H., (2017). The effects of Mach number on the flow separation control of airfoil with a small plate near the leading edge. *Computers & Fluids*, *156*(1), pp.274-282. https://doi.org/10.1016/j.compfluid.2017.07.014.